

MUHD: A Multi-channel Ultrasound Prototype for Remote Heartbeat Detection

S. Franceschini^a, M. Ambrosanio^b and F. Baselice^c
Department of Engineering, University of Naples Parthenope, Naples, Italy

Keywords: Ultrasound System, Heartbeat Detection, Bio-radar.

Abstract: This paper presents a novel system based on ultrasonic waves that is capable of detecting heartbeat in a contactless fashion. The aim of this work is to design, build and test a prototype that could be effective, simple in its realisation and use and with a low cost of production. The idea is to exploit the displacement of the skin related to cardiac activity, that is possible by using phase difference between a transmitted wave and the waves resulting from the interaction with the subject skin. Nevertheless, this type of procedure is not new in the scientific literature, but in this manuscript the authors contribution mainly consists in the implementation of a multi-channel architecture in order to overcome the well known “null-point” issue. Furthermore, an a-priori regularisation function is used for making the system more robust against noise and artifact. The performance of the prototype has been tested on volunteers and the results are quite close to standard electrocardiography used as reference.

1 INTRODUCTION

Remote sensing of human vital signs is of great interest since the second half of the 20th century (Masgram et al., 2009). The ability of detecting heartbeats and breath without any contact makes these technologies very attractive for several applications, such as occupancy sensing, identification devices, driver-health control and others. Among these parameters, heart rate (HR) is of great interest.

Nowadays the gold-standard in HR monitoring is the electrocardiogram (ECG), which consists in a measure of the electrical heart activity that rules the heartbeat. Even though it is very reliable, it has some drawbacks such as susceptibility to moving artifacts and the need of constant contact with subject’s skin, which might be annoying for long time monitoring, or simply impossible for some classes of patients (e.g., patients with burns or having allergies with electrodes or gel employed in the measure).

Several techniques have been developed for the remote monitoring of physiological parameters (Kranjec et al., 2014; Arcelus et al., 2013; Bonde et al., 2018). The cardiac activity can be detected basically

in two ways: directly or indirectly, i.e. measuring other parameters related to the heart activity. During its rhythmical activity the heart has some volumetric and pressure changes that cause waves propagating through the body. These mechanical waves are visible via sub-millimetre displacements of the skin, and usually are detected by very high resolution sensors often exploiting the Doppler effect (Droitcour et al., 2004). In the research community, articles based on electromagnetic (EM) radar devices for monitoring purposes are quite numerous (Suzuki et al., 2008; Obeid et al., 2010; Varanini et al., 2008). Although they can reach high-level performance, their use is limited by their cost, high susceptibility to external interference, high amount of EM energy required for the two-way path of the wave and the need of semi-fixed patients.

To overcome some of these issues, ultrasound (US) systems have been proposed (Min et al., 2010). These devices are cheaper than EM radars and free from interference with other electronic devices. US monitoring systems could be classified by their architecture, the most appropriated one is the short range continuous wave (CW) US radar (Kim and Nguyen, 2004; Gu et al., 2010; Droitcour et al., 2001). Unlike other approaches, this paper presents a multi-channel CW-US system that measures the phase difference between a transmitted and received wave. Conversely from the Doppler effect which allows a measure of

^a <https://orcid.org/0000-0002-7608-6686>

^b <https://orcid.org/0000-0003-3669-8183>

^c <https://orcid.org/0000-0002-5964-8667>

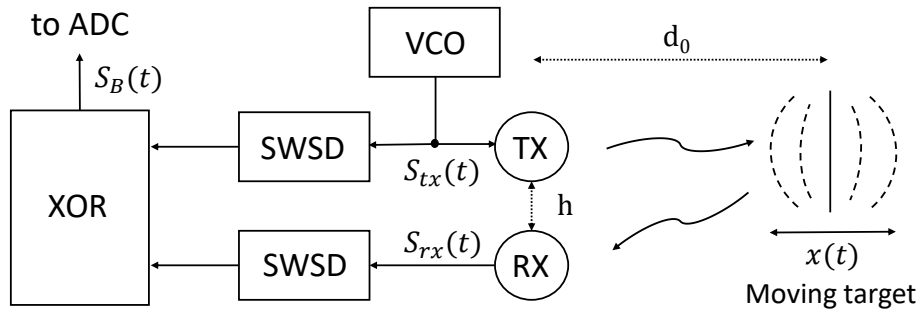


Figure 1: High-level sketch of a possible architecture of CW US system for the detection of moving targets. VCO: voltage-controlled oscillator, TX: transmitting sensor, RX: receiving sensor, SWSD: square-wave shaping detector, XOR: exclusive OR logic port, ADC: analog-to-digital converter.

skin-movement velocity, the proposed system measures its displacement. The choice of using different channels is related to the need of overcoming the null-point issue addressed in Section 2. Moreover the system uses an a-priori-based detection strategy which makes the measures more robust against noise and artifacts.

The remainder of the paper is as follows: Section 2 provides some details regarding the physical model, while Section 3 is focused on the technical hardware used for the prototype realisation. The description of the idea behind the software implementations are shown in Section 4, in the same Section a protocol applied on some volunteers and some results are shown. Finally, some conclusions end the paper.

2 THEORETICAL MODEL

The main idea of this system is to exploit a secondary effect of the cardiac activity for the heartbeat detection. During its rhythmical beating, the heart produces pressure variations in near tissues causing pressure waves that propagate until the skin. Thus, as a consequence of the heartbeat, tiny vibrations are observable in regions near to the main human pressure points. Considering the chest area, these vibrations are typically between 0.2 and 0.5 mm with a frequency between 1 and 2 Hz. It is important to notice that the same region is also affected by the respiration activity that is responsible of a 4-12 mm vibration in a frequency range [0.1, 0.3] Hz (Konno and Mead, 1967; Massaroni et al., 2018b; Hassan et al., 2017; Massaroni et al., 2018a). Providing useful information from the movement of the skin is not easy both for the superimposed presence of the breathing activity as well as for the weak vibrations to be detected. Another issue is related to the undesired movements of the patients that may worsen the quality of the

measures. Regarding the useful regions for collecting the heartbeat information, an interesting region is the pit of neck which seems to be a valid alternative to the standard chest area (Silbernagl and Despopoulos, 2015).

Although the detection of sub-millimetre movements is quite challenging, a good option for its detection could be the use of a continuous-wave ultrasound (CW-US) system with a possible architecture presented in Fig. 1. A sinusoidal wave is provided by a voltage-controlled oscillator (VCO) and travels through the air reaching the region of interest, and then goes back as back-scattered modulated wave. If the target is moving, the reflected wave has some phase variations. By comparing the transmitted and received waves, and extracting the phase variation with a non-linear procedure, the system is capable of providing information regarding the heart activity. Referring to a model with the transmitter in front of the target and a receiver aligned to the subject, it is possible to write the transmitted wave $S_{tx}(t)$ as:

$$S_{tx}(t) = A_{tx} \cdot \cos[2\pi f_c t + \phi_n(t)], \quad (1)$$

where f_c is the carrier frequency, A_{tx} is the signal amplitude and $\phi_n(t)$ is the phase noise of the VCO. The reflected wave is multiplied by the transmitted one and then low-pass filtered. The base-band output $S_B(t)$ can be expressed as:

$$S_B(t) \approx A \cdot \cos \left[k + \beta_c \cdot \left(1 + \frac{d_0}{\sqrt{h^2 + d_0^2}} \right) \cdot x(t) + \Delta\phi_n(t) \right], \quad (2)$$

with A amplitude of the base-band signal, $\beta_c = 2\pi/\lambda_c$, λ_c is the carrier wavelength, d_0 is the mean distance between the transmitter and the target, $x(t)$ is the radial movement of the skin which is, in our case, the quantity of interest, $\Delta\phi_n(t)$ is the residual noise, h is the distance between transmitter and receiver, and k is a constant quantity related to β_c , d_0 and h .

If the target is quite near to the transmitter, the phase noise of the reflected signal is almost equal to the one of the local oscillator, so by mixing both signals the residual phase $\Delta\theta_n(t)$ is usually negligible. Since the displacement is very small compared to the wavelength, if k is an odd multiple of $\pi/2$, the base-band output $S_B(t)$ becomes approximately linear respect to the quantity $x(t)$, which represents the optimal case; conversely, if k is an even number of multiples of $\pi/2$, the output signal is not linear anymore to the cardiac information and this represents the worst case, which is known as “null-point” and makes the measures very inaccurate. Since the working point depends on k , which is related to the target distance, the null-point problem occurs every $\lambda_c/4$.

For addressing this issue, several techniques have been proposed as in (Xiao et al., 2006) and (Droitcour et al., 2004). Our solution is designed to be cheap and technologically easy to be implemented since it is based on the spatial diversity of different receivers positions. All the receivers, being placed at a different distance from the transmitter (i.e., different h values), they receive different signals which yields to different phase terms.

The distance has to be chosen properly in order to allow the system to be capable of using at least one channel in every situation. The right distances are the ones that guarantee to avoid the simultaneous presence of null-points in all channels. In the following section, more details about the hardware and software design of the prototype will be provided.

3 PROTOTYPE DEVELOPMENT

The proposed system is a coherent CW-US system which has been tested in numerous cases, both on moving phantoms as well as on human volunteers in a laboratory-controlled scenario. The transmitted signal is a cosine at frequency of 40 kHz. Being the wave transmitted in air, its velocity is approximately equal to 343 m/s, with a wavelength of approximately 8 mm; therefore, the maximum allowed displacement is equal to 4 mm and larger movements will result in a non-unique solution in the non linear demodulation. However, as shown in the Section 2, the displacement to be detected is lower than this value.

The active part of the system is the VCO which supplies the 40 kHz cosine used for the transmission. The amplitude voltage is fixed to the one that ensures safety values as sound pressure levels (SPL). More in detail, this value must be lower than 105 dB for a subject at a 30-cm distance in accordance with the International Commission on Non-Ionising Radiation

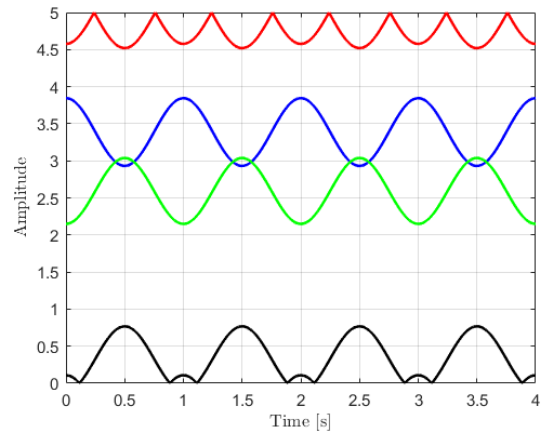


Figure 2: Numerical example of the null-point issue. Supposed a cosine-law displacement of the target, the channels in red and in black are affected by null points and the resulting signal is no more a cosine function.

Protection (ICNIRP) guideline (Jammet et al., 1984). Both the transmitted and back-scattered waves are then sent to a square-wave shaping detector (SWSD) and converted into square waves with amplitude between 0 and 5 V. Finally, the signals are sent to an exclusive OR logic port (XOR) which provides a signal related to the phase difference between the transmitter and the receiver.

In case of no differences, the output will be 0 Volt; conversely, in case of a half-period delay the result will be 5 Volt (the maximum value). The former case results in a null output, which is the aforementioned null-point. A numerical example of the possible effect of the null point issue is shown in Fig. 2, in which the target is moving following a cosine law and the signal acquired by the red and black channels, which are effected by the null-point problem, are not cosines anymore.

A multi-channel system has been used to overcome this problem, which allows to record signals at different sensors locations. Therefore, if the null-point occurs in one channel, it is very unlikely that it will occur in all of them, having chosen the distances among transmitter and receivers properly. In particular, since our purpose at this step is a near range detection, the mutual distances between the transmitter and the receivers are 1.6, 2.0, 3.0, 3.5 cm for the red, green, violet and black-coloured sensors respectively. This particular configuration ensures that there is no null-point in all the four channels simultaneously if the target is nearer than 40 cm from the prototype. If the working distance increases, farther receivers locations must be considered.

Regarding the ultrasonic sensors, the models 40LT16 and 40LR16 manufactured by SensComp

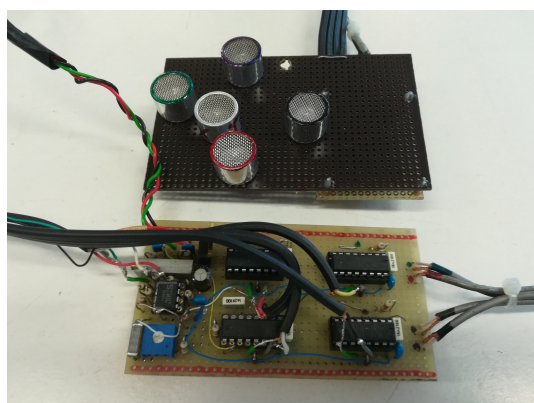


Figure 3: Picture of the prototype. In the top the board with the US sensors, in the bottom the board with the electronics.

were employed for the transmitter and receivers, respectively. These piezoelectric sensors have a quite narrow bandwidth of about 2 kHz centred at 40 kHz with a radiation pattern at -6 dB of approximately sixty degrees both in the horizontal and vertical axes. The SWSD electronics is mounted on one board, while OR logic ports and the electronic components are placed on a second board. A picture of the complete prototype is shown in Fig. 3. The output signal of the XOR port is sent to an analog-to-digital converter (ADC) which, in our case is a PCI-6251 board manufactured by National Instrument. This board has a 16-bit resolution and a maximum sample rate of 1.25 MS/s. For our measures, the sampling frequency was fixed at 200 Hz with sixteen-bit precision. A LabVIEW script was used to manage the acquisition routine. Once acquired, the signals are processed in Matlab (The Mathworks, Inc.).

4 DATA PROCESSING

In order to evaluate the capability of the prototype to detect the heartbeat, the system was firstly tested on moving phantoms and then on volunteers. The complete signal processing is a step-by-step procedure that aims at emphasising the heartbeat components in the acquired signals. In this section, some results and the procedure employed for the data processing are reported.

4.1 Acquisition Protocol

The prototype has been tested on 4 male volunteers, with an age between 30 and 60 years. Per each subject, two acquisitions of length 60 seconds of the cardiac signal were recorded. In all the cases the proto-

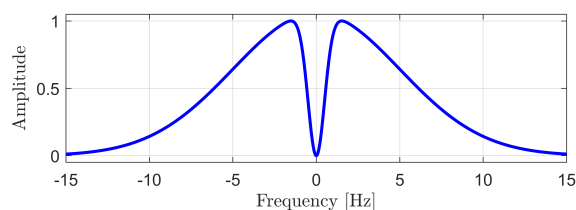


Figure 4: Band-pass Gaussian-shaped filter for cutting-off noise and breathing from the signal.

type was placed at 20-cm distance from the pit of the neck, considering this area as target area. All the measures were recorded in the same scenario and conditions. The volunteers laid down in a supine position, breathing normally and relaxed. During the acquisition, in order to evaluate the performance of the system, the ECG signal was also recorded. For this purpose, three electrodes were placed on left and right arms and on the right leg following the Einthoven's triangle. These electrodes are linked with a commercial electronic board which filters and amplifies the signal. The ECG signal is acquired with the same DAQ used for the US sensors, guaranteeing the simultaneity of all the signals.

4.2 Pre-processing

After acquiring the signals, a filter to cut-off noise and artifact effects is employed. More in detail, high-frequency noise and low-frequency residual breathing components are the main cause of signal degradation. For the data pre-processing, a modified Gaussian-shaped band-pass filter was employed whose frequency response is reported in Fig. 4. The bandwidth of this filter is [0.6, 6] Hz, which is a good compromise between preserving the useful component of the signal and reducing the amount of noise and breathing effect. Fig. 5 shows a portion of a recorded filtered US signal (in red) overlapped on the reference ECG signal (in blue). It is worth to note that the signal measured by the proposed US system has peaks which have a constant delay with respect to the ECG ones, and the reason is related to the fact that the two signals are different, since the former is mechanical, while the latter is electrical.

4.3 Detection Strategy

The pre-processed data is cut into pieces of equal length and filtered by means of a moving window. The length of the window is fixed and properly selected in order to have a region with the presence of only one peak with the highest probability. The peak is assumed to correspond to the maximum value in

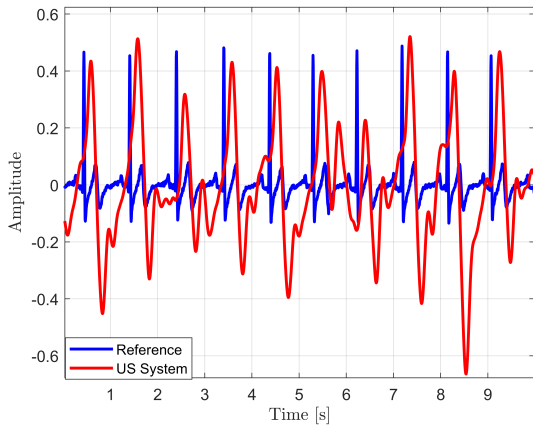


Figure 5: Plot of the reference ECG (blue) and filtered US (red) signals (ten-second length signals).

each window. It is worth to note that this strategy is an adaptive one, since after the detection of each heartbeat, the next window will be starting from the time instant at which the current heartbeat is estimated. For the heartbeat detection, a good value for window's width seems to be 1.25 s, which works quite well for healthy patients. However, in presence of two or more peaks closer than 0.5 second, the one with higher amplitude is selected. The length of the moving window, as well as the peak selection, are easily tunable in case of patients affected by bradycardia or tachycardia.

4.3.1 Best Channel Selection

The detection strategy proposed previously is characterised by different performance according to the considered channels. Therefore, it is worth to exploit an automatic strategy for selecting the best channel per each measure. To this aim, a two-step procedure was adopted. Firstly, the recorded signals whose amplitudes are close to the limits of the range [0, 5] Volt are discarded, since they are intrinsically not reliable. After that, the signal power in the frequency bandwidth [0.9, 1.2] Hz is estimated (which represents the useful bandwidth for healthy people). The higher the power, the higher the contribution of the cardiac signal is supposed to be in the overall acquired signal. This measure represents an indirect evaluation of the signal to noise (SNR) ratio, so the channel that has the highest value is selected for the heartbeat detection step.

4.3.2 A-priori Regularisation Window

Even though the automatic choice of the best channel assures that the detection step is performed on the channel with the highest SNR, artifacts and noise

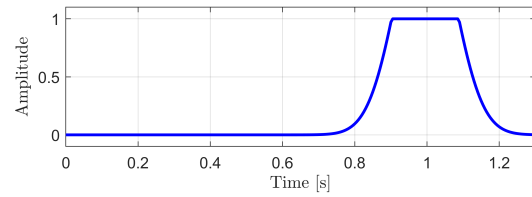


Figure 6: Clipped Gaussian-shaped window employed for the heartbeat detection step.

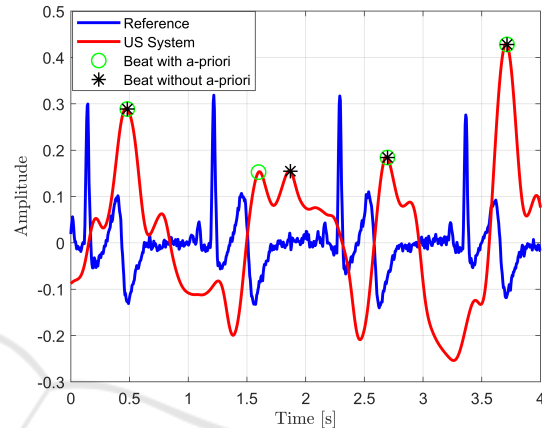


Figure 7: Effect of the regularisation window. In blue the reference signal, in red the US signal, the black stars represent the beats detected without the use of the a-priori function, while the green circles are the beats detected by employing the clipped Gaussian-shaped window.

might still be present in the measures. In order to make the detection step more robust, a clipped Gaussian-shaped window is employed. This regularisation window emphasises parts of the signal in which the peaks are expected to be located with higher probability. To this aim, every searching window is multiplied with this window centred at the expected position of the beat. This instant is calculated using the distance evaluated at the previous detected beat.

Fig. 6 shows an example of application of this window in case that the expected beat is centred at 1 second from the previous one. Fig. 7 illustrates a comparison of the heartbeat detection step by employing a clipped Gaussian-shaped function and without any prior information. It is clear from the figure that the detection strategy without the regularisation window is not able to properly identify the heartbeat peak.

4.4 Results

After the heartbeat detection step, an average BPM value was calculated per each case. A comparison between the average BPMs evaluated via standard ECG

Table 1: Mean of heartbeats [BPM] measured by the ECG and the proposed US system.

	Subject 1		Subject 2		Subject 3		Subject 4	
	Acq.1	Acq.2	Acq.1	Acq.2	Acq.1	Acq.2	Acq.1	Acq.2
ECG	64.10	65.55	57.28	58.04	67.30	70.07	56.74	63.83
US	64.10	65.55	57.28	58.18	67.42	70.09	56.80	63.89

and the ones by means of the prototype are presented in Table 1. The table shows that the results obtained by the proposed system are very similar to the ones obtained by reference ECG with a very low error (maximum absolute error of 0.12 s).

5 CONCLUSIONS

This manuscript presents a US prototype for non-contact heartbeat detection. The system measures skin displacement due to the pressure waves generated by the cardiac activity and exploits a multi-channel architecture to overcome the null-point issue and a windowing procedure for enforcing the heartbeat detection. The prototype was built and tested on four volunteers. Results are encouraging, as the system was able to provide a performance level in detecting heartbeats comparable to standard electrocardiography. Further work will focus on the improvement of system robustness to subject movements and external artifacts, as well as on increasing the working distance of the system.

ACKNOWLEDGEMENTS

The work has been partially supported by the funding program “Bando di sostegno alla ricerca individuale per il triennio 2015-2017” of the University of Napoli Parthenope.

REFERENCES

- Arcelus, A., Sardar, M., and Mihailidis, A. (2013). Design of a capacitive eeg sensor for unobtrusive heart rate measurements. In *2013 IEEE International Instrumentation and Measurement Technology Conference (I2MTC)*, pages 407–410.
- Bonde, A., Pan, S., Jia, Z., Zhang, Y., Noh, H. Y., and Zhang, P. (2018). Vvrrm: Vehicular vibration-based heart rr-interval monitoring system. In *Proceedings of the 19th International Workshop on Mobile Computing Systems & Applications*, pages 37–42. ACM.
- Droitcour, A., Lubecke, V., Lin, J., and Boric-Lubecke, O. (2001). A microwave radio for doppler radar sensing of vital signs. In *International Microwave Symposium Digest*, volume 1, pages 175–178. IEEE.
- Droitcour, A. D., Boric-Lubecke, O., Lubecke, V. M., Lin, J., and Kovacs, G. T. (2004). Range correlation and I/Q performance benefits in single-chip silicon doppler radars for noncontact cardiopulmonary monitoring. *IEEE Transactions on Microwave Theory and Techniques*, 52(3):838–848.
- Gu, C., Li, C., Lin, J., Long, J., Huangfu, J., and Ran, L. (2010). Instrument-based noncontact doppler radar vital sign detection system using heterodyne digital quadrature demodulation architecture. *IEEE Transactions on Instrumentation and Measurement*, 59(6):1580–1588.
- Hassan, M. A., Malik, A. S., Fofi, D., Saad, N. M., Ali, Y. S., and Meriaudeau, F. (2017). Video-based heart-beat rate measuring method using ballistocardiography. *IEEE Sensors Journal*, 17(14):4544–4557.
- Jammet, H. P., Bosnjakovic, B. F. M., Czerski, P., Faber, M., Harder, D., Marshall, J., Repacholi, M. H., Sliney, D. H., and Villforth, J. C. (1984). Interim guidelines on limits of human exposure to airborne ultrasound. international non-ionizing radiation committee of the international radiation protection association. *Health Physics*, 46:969–974.
- Kim, S. and Nguyen, C. (2004). On the development of a multifunction millimeter-wave sensor for displacement sensing and low-velocity measurement. *IEEE Transactions on Microwave Theory and Techniques*, 52(11):2503–2512.
- Konno, K. and Mead, J. (1967). Measurement of the separate volume changes of rib cage and abdomen during breathing. *Journal of applied physiology*, 22(3):407–422.
- Kranjec, J., Begus, S., Drnovsek, J., and Gersak, G. (2014). Novel methods for noncontact heart rate measurement: A feasibility study. *IEEE Transactions on Instrumentation and Measurement*, 63(4):838–847.
- Massagram, W., Lubecke, V. M., and Boric-Lubecke, O. (2009). Microwave non-invasive sensing of respiratory tidal volume. In *Annual International Conference of Engineering in Medicine and Biology Society*, pages 4832–4835. IEEE.
- Massaroni, C., Lopes, D. S., Lo Presti, D., Schena, E., and Silvestri, S. (2018a). Contactless monitoring of breathing patterns and respiratory rate at the pit of the neck: A single camera approach. *Journal of Sensors*, 2018.
- Massaroni, C., Venanzi, C., Silvatti, A. P., Lo Presti, D., Saccomandi, P., Formica, D., Giurazza, F., Caponero, M. A., and Schena, E. (2018b). Smart textile for respiratory monitoring and thoraco-abdominal mo-

- tion pattern evaluation. *Journal of biophotonics*, 11(5):e201700263.
- Min, S. D., Kim, J. K., Shin, H. S., Yun, Y. H., Lee, C. K., and Lee, M. (2010). Noncontact respiration rate measurement system using an ultrasonic proximity sensor. *IEEE Sensors Journal*, 10(11):1732–1739.
- Obeid, D., Sadek, S., Zaharia, G., and El Zein, G. (2010). Multitunable microwave system for touchless heartbeat detection and heart rate variability extraction. *Microwave and optical technology letters*, 52(1):192–198.
- Silbernagl, S. and Despopoulos, A. (2015). *Color Atlas of Physiology*. Thieme.
- Suzuki, S., Matsui, T., Imuta, H., Uenoyama, M., Yura, H., Ishihara, M., and Kawakami, M. (2008). A novel automatic activation measurement method for stress monitoring: non-contact measurement of heart rate variability using a compact microwave radar. *Medical & biological engineering & computing*, 46(7):709–714.
- Varanini, M., Berardi, P., Conforti, F., Micalizzi, M., Neglia, D., and Macerata, A. (2008). Cardiac and respiratory monitoring through non-invasive and contactless radar technique. In *Computers in Cardiology*, pages 149–152. IEEE.
- Xiao, Y., Lin, J., Boric-Lubecke, O., and Lubecke, M. (2006). Frequency-tuning technique for remote detection of heartbeat and respiration using low-power double-sideband transmission in the Ka-band. *IEEE Transactions on Microwave Theory and Techniques*, 54(5):2023–2032.

